Journal of Chromatography, 517 (1990) 31–49
Elsevier Science Publishers B.V., Amsterdam

CHROMSYMP. 1980

Dispersion in the interstitial space of packed columns

PIERRE MAGNICO and MICHEL MARTIN*
École Supérieure de Physique et Chimie Industrielles, Laboratoire de Physique et Mécanique des Milieux Hétérogènes, URA CNRS 857, 10 rue Vauquelin, 75231 Paris Cedex 05 (France)

ABSTRACT

In order to study the dispersion mechanism occurring in the interstitial space of a porous medium, a column was packed with large (210 μm) impenetrable particles by a special dry-packing procedure, designed to obtain a permeable bed that is as uniform as possible. The experimental conditions are selected so as to eliminate as far as possible any other source of dispersion and focus essentially on that arising in the moving fluid. A linear regression analysis of the dispersion data for non-retained solutes shows that the Huber and the Horváth and Lin models fail to describe correctly the experimental results whereas the Giddings model provides a good fit to the data. The reduced plate height becomes constant and equal to 2 at high reduced velocities. It reaches a minimum value of 1 at a reduced velocity of about 3. The models and some previously published experimental data are discussed at the light of these results.

INTRODUCTION

The quality of chromatographic resolution depends on the extent of the broadening of the individual component zones as much as on the retention gap between adjacent zones. The control of this zone broadening, and hence of the dispersion of the zones as they migrate along the chromatographic column, has always been an essential goal in optimization studies of chromatographic separations. The zone dispersion in the column is due essentially to two broad classes of phenomena: (i) longitudinal molecular diffusion as a result of longitudinal solute concentration gradients and (ii) resistance to mass transfer between regions of the cross-section with different velocity components along the direction of flow. The former depends essentially on the time spent by the solute in the column. The latter can occur because of the retention of the solute on, or in, a stationary phase or because of the presence of a stagnant region of the mobile phase inside the pores of the particles. The contribution to the band broadening arising from these different sources is relatively well documented, especially when one is specifically concerned with their dependence on the carrier flow-rate. Flow non-uniformities in the cross-section of the column are also present in the interstitial space between the particles because of the shear forces

0021-9673/90/$03.50

associated with the viscous flow and of the more or less erratic path followed by the flow streamlines in the complex geometry of the porous bed. These flow inequalities contribute to the zone dispersion but the dependence of this contribution on the flow-rate is relatively complex. Several equations based on different approaches and differing mainly in the exponent of the velocity have been developed to account for this contribution. Exponents 1, 1/2 and 1/3 appear in the eddy diffusion coupling term of the models developed by Giddings[1], Huber and Hulsman[2,3] and Horváth and Lin[4], respectively. In spite of the practical importance of the corresponding term in the plate-height equation (it has a major influence on the coordinates of the minimum of the Van Deemter curve), no definitive proof of the correctness of any of these models can yet be established from experimental liquid chromatographic measurements as various and sometimes conflicting conclusions about this contribution have been derived by different authors.

It seems that these discrepancies arise mainly because the relatively slight differences between the three models are obscured by other contributions to band broadening (resistance to mass transfer in the stagnant carrier fluid within the pores of the particles or in the stationary phase, influence of retention on dispersion, extra-column band broadening) or because it was erroneously assumed that the dispersion coefficient was constant along the column whereas, in fact, a length-averaged coefficient is experimentally measured. This might be the case in liquid chromatography with packings of small particles as the relatively large pressures applied at the column inlet may affect the values of the diffusion coefficients. Further, under these conditions, the radial dissipation of the heat generated by the friction of the liquid on contact with the particles induces a radial viscosity profile and, consequently, a velocity profile which contributes to the broadening of the zones. Preliminary calculations indicate that the contribution of this effect to the plate height might increase with the fifth power of the velocity for a fully developed temperature profile[5].

The aim of this study was to determine the best model describing the physical dispersion process occurring in the interstitial space of the chromatographic packing. The experimental conditions are designed so as to focus essentially on this source of band broadening by eliminating, as far as possible any other contribution to the dispersion, except, of course, the irreducible longitudinal molecular diffusion. These conditions include the use of sieved, impervious and spherical particles, very low pressure drops, non-retained solutes and a packing procedure that provides a packing that is as regular as possible. Special attention was paid to the column arrangement to avoid any disturbing fluid instability and to the initial filling of the packing by the liquid to ensure that no air pockets remain entrapped within the packing.

THEORY

If structural heterogeneities present in the porous medium have a length scale which is small in comparison with the column length, the dispersion of the solute is described by the classical convection–diffusion equation:

$$\frac{\partial c}{\partial t} + U \cdot \frac{\partial c}{\partial x} = D \cdot \frac{\partial^2 c}{\partial x^2} \tag{1}$$

which is a combination of the phenomenological Fick's law and of the mass conservation law. Although dispersion occurs in all directions, one is concerned here only with dispersion along the longitudinal flow direction. The variable x is the distance along the column from the inlet, t the time, U the mean mobile phase velocity, c the cross-sectional average concentration of the solute and D the overall solute dispersion coefficient. In order for these terms to be defined, one has to assume the existence of a scale beyond which the porous medium is homogeneous, *i.e.*, the variables c, U, D and x are averaged over a volume known as the representative elementary volume, which must be of a small size compared with the column volume.

In the situation where one injects a continuous solution of solute with a concentration c_{max}, starting at time $t = 0$, at the inlet of the column previously filled with a solution of concentration c_{min}, which corresponds to the experimental set-up of this study, the limiting conditions for concentration in time and space are, respectively,

$$\Gamma(x,t = 0) = 0 \tag{2}$$

$$\Gamma(x = 0, t) = 1 \tag{3}$$

and, assuming a semi-infinite medium:

$$\Gamma(x \to \infty, t) = 0 \tag{4}$$

In these equations Γ is the dimensionless concentration $(c - c_{min})/(c_{max} - c_{min})$. The solution of eqn. 1 with these limiting conditions is[6]

$$\Gamma(x, t) = \frac{1}{2}\left[\operatorname{erfc}\left(\frac{x - Ut}{2\sqrt{Dt}}\right) + \exp\left(\frac{Ux}{D}\right)\operatorname{erfc}\left(\frac{x + Ut}{2\sqrt{Dt}}\right)\right] \tag{5}$$

which, when Ux/D is larger than 100, becomes, with a good approximation, equal to[6]

$$\Gamma(x, t) = \frac{1}{2}\operatorname{erfc}\left(\frac{x - Ut}{2\sqrt{Dt}}\right) \tag{6}$$

In eqns. 5 and 6, erfc represents the complementary error function. The approximation represented by eqn. 6 fully applies under the present experimental conditions where Ux/D lies in the range $2 \cdot 10^3$–$2 \cdot 10^6$ when x is taken as the column length.

The study of the dispersion of the solute reveals different properties of the medium depending on the flow-rate. When the mean velocity is very low, the solute dispersion is the same as the molecular diffusion which would be observed if a concentration gradient of the solute was established between the inlet and the outlet of the column without flow. The dispersion coefficient, D, measured is then proportional to the molecular diffusion coefficient, D_m and

$$D = \frac{D_m}{T} \tag{7}$$

The factor T is known as the tortuosity and is larger than 1. The tortuosity can be determined by measurements of the electrical conductivity of the packing. It is found that, in the porosity range encountered in bead packings, $T \approx \varepsilon^{-1/2}$, where ε is the porosity of the packing[7,8].

When the carrier flow-rate increases, the dispersion coefficient is no longer constant but becomes a function of the mean velocity. More generally, this function depends on the dimensionless reduced velocity, or Péclet number, Pe, which is the ratio of the times required to transport the solute along one particle by diffusion and by convection:

$$Pe = \frac{d_p^2/D_m}{d_p/U} = \frac{Ud_p}{D_m} \tag{8}$$

where d_p is the particle diameter and U the mean velocity.

It is convenient to express the dispersion in terms of the dispersion length, L_d:

$$L_d = D/U \tag{9}$$

This length represents half the plate height frequently used in the field of separation science.

Various equations, or models, have been proposed to represent the dependence of the dispersion length on the operational parameters and, especially, the carrier velocity. The models relevant in the context of this study are presented below assuming that there is no interaction of the solute with the packing, *i.e.*, no retention, and that the packing is made of impervious rigid spheres (no internal pores). Accordingly, dispersion will only occur in the space occupied by the carrier fluid between the particles and, apart from the molecular diffusion term arising from the existence of a longitudinal concentration gradient and expressed by the eqn. 7, is due to flow variations associated with structural heterogeneities of this space.

The Giddings model

The velocity field in a packed bed is much more complex than that in a capillary tube. Consequently, apart from the Taylor-like dispersion arising in an interstitial flow channel because of the transversal velocity variations within this channel, solute dispersion can also come from the erratic flow pattern associated with the presence of a more or less regular array of particles. These two kinds of dispersion processes can be called hydrodynamic dispersion and geometric (or mechanical) dispersion, respectively. One notes in passing that the latter process is also known as the anastomosis and, more commonly in the chromatographic literature, as the "eddy diffusion", a term which we prefer to avoid as it has mistakenly been associated in the past by some authors with the eddies induced by a turbulent flow. Clearly, the geometric dispersion mechanism appears in the laminar flow regime at low values of the Reynolds number.

The influence of these two kinds of dispersion was recognized in one of earliest models of peak broadening in chromatography by Van Deemter *et al.*[9], who simply added their respective contributions to the dispersion length. Later, this model was modified by Giddings[1], who noted that these contributions are not independent and thus additive but, instead, are coupled.

In this model, five different levels of flow heterogeneities are considered for packings of porous particles[1]. In the present study dealing with non-porous particles packed by a special procedure to ensure a packing as regular as possible, one will be concerned mainly with the trans-channel level and, to a lesser extent, with the short-range inter-channel level. The characteristic length scale of these velocity variations is assumed to be proportional to the particle diameter.

This model assumes that the dispersion due to the velocity variations is similar to a random walk process. The time corresponding to an elementary step, or correlation time, is defined as the time necessary for a solute molecule to travel from one velocity domain to another. Two mechanisms allow this transport, molecular and convection, which both have a specific correlation time. The corresponding dispersion lengths $L_{d,hydro}$ and $L_{d,geo}$ for the diffusive (hydrodynamic dispersion) and convective (geometric dispersion) mechanisms are, respectively,

$$L_{d,hydro} = C \cdot \frac{d_p^2 U}{D_m} \tag{10}$$

$$L_{d,geo} = \Lambda d_p \tag{11}$$

where Λ and C are dimensionless parameters which depend on the scale and amplitude of flow non-uniformities.

Basically, the coupling theory assumes that the total numbers of steps in the random walk is the sum of the number of steps for each of the individual processes. Then, the resultant correlation time and the resultant dispersion length appear to be the harmonic, rather than the arithmetic, sum of their respective individual contributions. Accordingly, the overall dispersion length is, combining eqns. 7, 9, 10 and 11:

$$L_d = \frac{D_m}{TU} + \frac{1}{\dfrac{1}{\Lambda d_p} + \dfrac{D_m}{C d_p^2 U}} \tag{12}$$

or

$$l_d = \frac{L_d}{d_p} = \frac{1}{TPe} + \frac{1}{\dfrac{1}{\Lambda} + \dfrac{1}{CPe}} \tag{13}$$

where l_d is the reduced dispersion length, which is half the reduced plate height. In these equations, the individual contributions of the longitudinal concentration gradient and transversal flow non-uniformities to the dispersion length have been added as they act independently to disperse the solute. At large values of the Péclet number, the dispersion is controlled by the convective mechanism and then the coupling term becomes constant while the diffusive process is dominant at lower Pe values.

The Huber model

A model based on the mass balance equation was developed by Huber and

Hulsman[2,3]. It uses a correlation obtained through dimensional analysis of experimental data by Hiby[10] to express the dispersion term arising from the flow non-uniformities, which gives

$$L_d = \frac{D_m}{TU} + \frac{1}{\dfrac{1}{\Lambda d_p} + \dfrac{D_m^{1/2}}{C d_p^{3/2} U^{1/2}}} \tag{14}$$

or

$$l_d = \frac{1}{TPe} + \frac{1}{\dfrac{1}{\Lambda} + \dfrac{1}{CPe^{1/2}}} \tag{15}$$

This equation differs from the Giddings equation by the exponent 1/2 of the Péclet number in the last term and in the numerical value of the dimensionless coefficient C.

The Horváth and Lin model

The dispersion model developed by Horváth and Lin is based on the postulate that a stagnant layer of fluid surrounds the particles and occupies a fraction of the interstitial fluid volume[4]. According to the free surface theory of Happel[11] and Pfeffer and Happel[12], the thickness of this layer is proportional to $Pe^{-1/3}$.

The model assumes that the peak broadening of a non-retained solute is due to the geometric dispersion process during the flow-dependent time spent by the solute in the streaming part of the carrier fluid, which gives for the complete dispersion length expression

$$L_d = \frac{D_m}{TU} + \frac{1}{\dfrac{1}{\Lambda d_p} + \dfrac{D_m^{1/3}}{C d_p^{4/3} U^{1/3}}} \tag{16}$$

or

$$l_d = \frac{1}{TPe} + \frac{1}{\dfrac{1}{\Lambda} + \dfrac{1}{CPe^{1/3}}} \tag{17}$$

It also differs from the Giddings equation by the exponent of the Péclet number in the second term on the right-hand side and in the numerical value of the dimensionless coefficient C. It must be clear that, in spite of the close similarity of eqns. 13 and 17, the latter is not based on a coupling effect and completely neglects the diffusive transport mechanism in the second term due to the velocity unequalities. Nevertheless, it is interesting that, if one wants to modify the Horváth and Lin model by introducing a coupling effect between the diffusive process in the stagnant layer and the convective process either in the whole interstitial fluid or only in its streaming part, by the

harmonic addition of the corresponding correlation times, one obtains an expression which has exactly the form of eqn. 14, obviously with different values of the dimensionless coefficients A and C. Moreover, as indicated by Horváth and Lin in the note added in the proof of their paper[4], the same form is found if one includes in the dispersion length expression the additional, and independent, peak broadening contribution due to diffusion into the stagnant layer by properly taking into account the flow-dependent "capacity factor" which reflects the distribution of the solute between the streaming and stagnant parts of the interstitial fluid (however, we found a term which is numerically three times smaller than that of Horváth and Lin).

More recently, Koch and Brady[13] derived the dispersion coefficient associated with the presence of a boundary layer around the particles, which, according to Acrivos and Taylor[14], is also found to have a thickness proportional to $Pe^{-1/3}$, and obtained a dispersion length expression which is a linear function of ln Pe. Such an ln U dependence was previously obtained by Saffman[15] using a different model.

The Bouchaud and Georges model

A general theory of the dispersion of solute species due to the spatial fluctuations of the velocity field has been recently developed by Bouchaud and Georges[16] by means of models with a very simple geometry. In order to study the dispersion due to flow inhomogeneities in a porous medium, they use the idealized model represented in Fig. 1, which consists of a succession of identical cells in series. In each cell, two flow paths of different lengths and permeabilities are connected in parallel. Let V and γV be the velocities in the fast and slow branches of lengths ξ and $\lambda\xi$, respectively ($\gamma < 1$). A solute molecule entering a given cell has a probability P of entering the slow branch in which its mean residence time is $<\tau>$, while the time spent in one fast branch is simply ξ/V. Assuming that the dispersion process is ergodic, *i.e.*, that the time spent in a given region is proportional to the volume of this region, a relationship is found between the probability P, $<\tau>$ and the volume fraction f of the slow branches. Using a statistical approach, Bouchaud and Georges derived a general expression for the dispersion length in terms of the first and second moments of the distribution law of the residence times in the slow paths.

A particular expression is found in the case where the residence time is unique, which corresponds to a Dirac distribution. According to this model, each path does not contribute to the dispersion, but the overall dispersion of the transit times along a large number of cells arises from combination of the paths followed by a molecule,

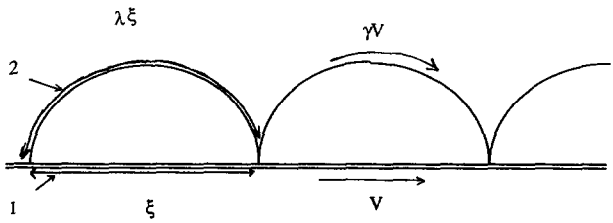

Fig. 1. Schematic model suggested by Bouchaud and Georges[16]. Two channel types (branches) are connected in parallel in one of a succession of cells connected to each other cell in series. In channel 1 of length ξ, the microscopic velocity V leads the transport process whereas, in channel 2 of length $\lambda\xi$, the local velocity γV ($\gamma < 1$) and the molecular diffusion both control the solute transport.

which is described by a binomial law. This model has been extended by Bouchaud[17] to the case where τ, the constant residence time in a slow branch, is the result of the combination of the diffusive and connective transport processes according to the harmonic coupling law:

$$\frac{1}{\tau} = \frac{2D_m}{\lambda^2 \xi^2} + \frac{\gamma V}{\lambda \xi} \tag{18}$$

Using the relationship between U, the average migration velocity of a solute molecule along the cell pattern, and V resulting from the ergodicity hypothesis, the dispersion length is found in the limit of large cell numbers and for an equal path length of the two branches ($\lambda = 1$):

$$L_d = \frac{D}{U} = \frac{1}{\dfrac{2\gamma}{\xi f(1-f)} + \dfrac{4D_m}{\xi^2 f U}} \tag{19}$$

or

$$l_d = \frac{L_d}{\xi} = \frac{1}{\dfrac{2\gamma}{f(1-f)} + \dfrac{4}{fPe}} \tag{20}$$

if the Péclet number is defined as $U\xi/D_m$. These equations do not include the longitudinal molecular diffusion term. However, regarding the more important term, in the present context, due to flow inequalities, they are similar to the corresponding Giddings' equations as far as the U dependence of the dispersion length is concerned. Clearly, this is due to the similarity of the ways in which the coupling between the diffusive and convective transports are introduced in the two approaches. However, eqns. 19 and 20, corresponding to the idealized, very simple geometric model represented in Fig. 1, show that when such a coupling occurs at a microscopic level (the individual slow branch), it manifests itself in the dispersion process at the macroscopic level. Further the Bouchaud and Georges model provides a physical meaning for the numerical coefficients which enter the dispersion equation. This is especially true for packings of porous particles.

EXPERIMENTAL

Packing procedure

A 16.6 cm × 2.4 cm I.D. column was packed with the 200–220-μm sieving fraction of glass beads by a special dry packing procedure designed to obtain a porous bed that is as regular as possible (Fig. 2). A vibrating distributor induces a constant flow of particles falling onto a short column packed with large (5 mm I.D.) glass beads, which ensures a homogeneous distribution of the particles across the whole cross-section. Then the particles pass through a set of parallel, vertical, 2.5 mm I.D. tubes, which help to keep the particles flowing homogeneously in the whole

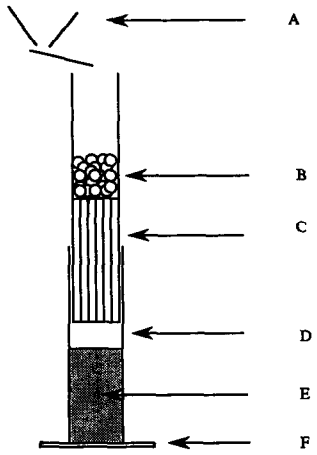

Fig. 2. Experimental set-up for column packing. A = hopper pouring the particles at a constant flow; B = packing of 5-mm glass beads; C = fixed set of 2.5 mm I.D. tubes; D = column section being packed; E = column section already packed with particles; F = support which allows the column to move and rotate around its axes.

cross-section of the packing assembly, before falling into the column to be packed. This column is moved down during the packing process in such a way as to maintain a constant falling height and avoid the formation of a longitudinal permeability gradient. At the same time, the column is rotating around its axis in order to avoid radial stratification of the packing.

Materials and methods

In order to avoid any trapping of bubbles which may significantly affect the dispersion process, the column, vertically orientated, is completely saturated with carbon dioxide, then filled upwards with water until the signal of an electrical conductivity cell monitoring the acidification of the water effluent due to the dissolution of the carbon dioxide bubbles becomes negligible. The volume of liquid in the column is of 28.5 cm^3, which gives a porosity of 38.0%. This porosity value considerably exceeds the corresponding value (26%) for a dense and perfect crystal-like arrangement of identical spheres but lies well within the range of porosities experimentally obtained when randomly packing by various techniques a very large number of particles (here about 10^7). It is believed that the packing procedure used in this study leads to a packing that is as uniform as possible.

Dispersion measurements are performed by frontal analysis of a solution of a mixture of NaCl and $CaCl_2$, rather than of a single salt solution, for eliminating ion exchange between the glass beads and the solution. A relative high concentration in the initial solution (0.5 g/l NaCl, 0.5 g/l $CaCl_2$) is used in order to avoid further adsorption and ion exchange of the solute mixture, which would otherwise lead to retention and to a significant effect on the profile, as previously observed. Then, a continuous step of solution at a different salt concentration is introduced in the column by switching the pump head of a dual-piston syringe pump (Model 919, Harvard Apparatus, South

Natick, MA, U.S.A.) by means of a four-way switching valve. The flow-rate range investigated was 33 μl/min–20 ml/min, which corresponds to Péclet numbers between 0.5 and 300. The pressure drop in the column was always less than 0.2 bar. In all instances the Reynolds number was lower than 0.4, which prevents any dispersion perturbation associated with the onset of turbulence.

The displacing solution is made more concentrated (1 g/l NaCl, 1 g/l $CaCl_2$ aqueous solution) than the initial solution to avoid the viscous fingering effect (Saffman–Taylor instability) which may occur when a more viscous solution is displaced by a less viscous solution. Further, the liquid moves upwards, rather than downwards, in order to avoid the Rayleigh–Taylor instability associated with the presence of a denser solution above a lighter one. These precautions are necessary with the relatively high concentration used in this study as these two effects have been shown to induce both an increase in the dispersion coefficient and a characteristic tailing of the elution profiles.

The concentration change of the column effluent is continuously monitored by a conductivity detector (Model 30063, Dionex, Sunnyvale, CA, U.S.A.). The temperature of the effluent is also measured in order to take into account the temperature dependence of the conductivity (2%/°C around 20°C), especially for the slowest analyses. The total dead volume of the pre- and post-column connecting capillary tubes, of the flow distributor and collector located at the column extremities and of the conductivity cell is 0.28 cm^3, *i.e.*, about 1% of the liquid volume in the column.

In the calculations, the particle diameter is assumed to be equal to 0.021 cm and $1/T$ equal to 0.6. The diffusion coefficient, D_m, is taken as equal to $1.336 \cdot 10^{-5}$ cm^2/s, which corresponds to the average of the individual coefficients of the two salts[18]. For dispersion coefficient determinations, the step between the two plateaux is normalized between 0 and 1 and measurements are performed in the 5–95% range of the front. At each time in this range, the experimental normalized concentration value gives, using eqn. 6 and the tabulated error function, the value of the reduced parameter $X = (L - Ut)/2\sqrt{Dt}$, where t is the elution time. Plotting $X\sqrt{t}$ *vs.* t gives a straight line for a Gaussian curve. The dispersion coefficient is obtained by linear regression from the intercept of this plot and the mean velocity from the slope. This mean least-square method of determination of D has the advantage of taking into account all experimental data for the front in the 5–95% range of the concentration step rather than the peak width at some more or less arbitrary selected concentration level, as classically performed in the small-pulse injection method.

RESULTS

The results obtained experimentally by this procedure are reported in Fig. 3, which shows the plot of the reduced dispersion length, l_d, *vs.* the Péclet number on a logarithmic scale. This curve has the characteristic shape of the classical Van Deemter curves with a minimum at a Péclet number of *ca.* 3 for a reduced dispersion length of about 0.5. This corresponds to a reduced plate height of 1, which is lower than that usually observed in packed chromatographic columns. Clearly, this low value is due to the use of impervious particles and to the quality of the homogeneity of the packing. With increasing Péclet number the dispersion length increases until it reaches a constant value of about 1 at large Péclet numbers.

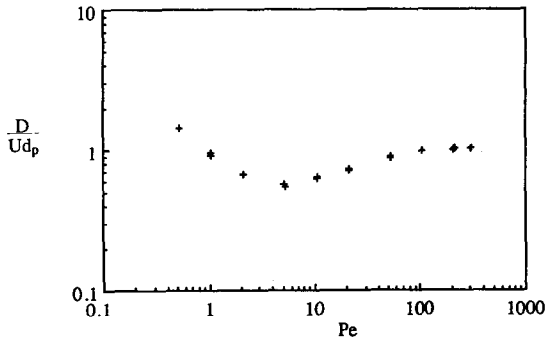

Fig. 3. Log–log plot of the reduced dispersion length *versus* Péclet number for a 16.6 cm × 2.4 cm I.D. column packed with 210-μm glass beads.

The models described above all predict a constant l_d value at large velocities, as observed, but they differ essentially in the exponent of the velocity in the hydrodynamic dispersion term of the dispersion length equation. The various equations can all be expressed by the following form:

$$\frac{D}{U} = \frac{D_m}{TU} + \frac{1}{\frac{1}{A} + \frac{1}{BU^n}} \tag{21}$$

with $n = 1/3$, $1/2$ and 1 for the Horváth and Lin, Huber and Giddings (or, equivalently, Bouchaud and Georges) models, respectively. The parameter $A = \Lambda d_p$ represents the convective (geometric) dispersion process for the three models (eqns. 12, 14 and 16). It is the limiting value of the dispersion length for large velocities. The B coefficient, taking into account the hydrodynamic dispersion, differs from one model to another. Looking for a linear relationship as an easy visual, and also quantitative, test to check the validity of the agreement between experimental (D, U) data and the theoretical expressions described above, one can transform eqn. 21 as follows:

$$Y = \frac{U^n}{A} + \frac{1}{B} \tag{22}$$

where Y is defined as:

$$Y = \frac{U^{n+1}}{D - \frac{D_m}{T}} \tag{23}$$

Then a plot of Y vs. U^n should give a straight line if the corresponding model is correct. These plots are shown in Fig. 4 for the three values of n. In these plots, only data points corresponding to Péclet numbers larger than 1 are used in order to reduce the influence

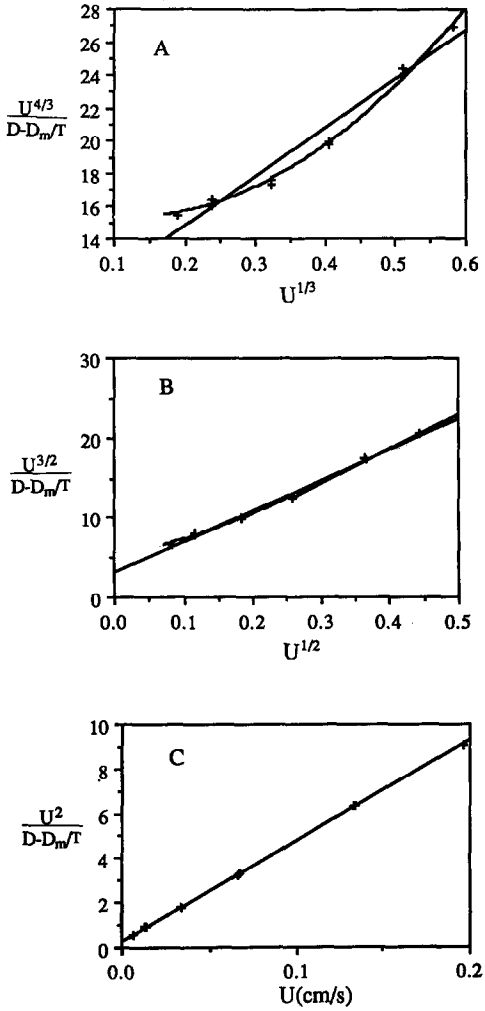

Fig. 4. Y *vs.* X plots of the experimental dispersion data with $X = U^n$ and $Y = U^{(n+1)}/(D - D_m/T)$. (A) $n = 1/3$; (B) $n = 1/2$; (C) $n = 1$. The straight lines correspond to mean least-square linear regressions. The other curves correspond to a second-degree polynomial fit.

of the uncertainties in the values of D_m and T on the denominator $(D - D_m/T)$. The best mean least-square linear fits are also indicated for each plot. Although, for the three curves, a monotonous increase of Y with U^n is observed, as expected from eqn. 22, it clearly appears that a remarkably good linear fit is obtained for $n = 1$, while the curve for $n = 1/2$ is slightly concave and at for $n = 1/3$ has a still more pronounced concavity.

As only one value of n can correctly describe the experimental data and as $n = 1$ appears to be the best of the three tested values, one cannot expect the plots for the two other n values in Fig. 4 to be straight lines. It is therefore of interest to check the

coherence of the shapes of the curves in Fig. 4, *i.e.*, to check that the observed shapes of the curves in Fig. 4A and B are in agreement with the shape that takes the theoretical variation corresponding to $n = 1$, when it is plotted according to the transformation of eqns. 22 and 23 but with another value of the parameter n (we shall take $n = 1/3$ and $n = 1/2$). For $n = 1$, eqn. 22 becomes

$$\frac{U^2}{D - \frac{D_m}{T}} = \frac{U}{A} + \frac{1}{B} \tag{24}$$

Combining eqns. 23 and 24, one obtains

$$Y = \frac{X}{A} + \frac{1}{BX^{(1-n)/n}} \tag{25}$$

with

$$X = U^n \tag{26}$$

Eqn. 25 clearly shows that the Y *vs.* X curve should not be a straight line if $n \neq 1$. When $n < 1$, it has a minimum, for:

$$X_{opt} = \left(\frac{1-n}{n} \cdot \frac{A}{B}\right)^n \tag{27}$$

The shape of the Y *vs.* X curves should therefore be concave for $n < 1$, which is indeed what is observed in Fig. 4A and B. The linear regression of the data according to eqn. 23 for $n = 1$ gives $A = 0.022$ and $B = 3.40$ (all dimensional values are in c.g.s. units). With these values, eqns. 25 and 27 give $X_{opt} = 0.24$ and $Y_{opt} = 16$ for $n = 1/3$ and $X_{opt} = 0.081$ and $Y_{opt} = 7.3$ for $n = 1/2$. Although the number of experimental points at low velocities in Fig. 4 is too small to show definite evidence of the presence of a minimum in the plots for $n = 1/3$ and $n = 1/2$, the coordinates of the minima for the two curves correspond roughly to those of points obtained at low velocity, which again agrees with the fact that the best of the three n values is 1.

Of the three n values for which dispersion models have been developed, $n = 1$ appears to be the best. One may wonder, however, if another value of n, not necessarily corresponding to a previous model, could provide a still better fit of the experimental data according to eqn. 21. This can be done by writing this equation in the form

$$Z = \ln\left(\frac{U}{D - \frac{D_m}{T}} - \frac{1}{A}\right) = \ln\left(\frac{1}{B}\right) - n \ln U \tag{28}$$

Then, a plot of Z *vs.* $\ln U$ should give a straight line, the slope of which should be equal to n. In fact, such a plot is very sensitive to the value of A which has to be stated. This is

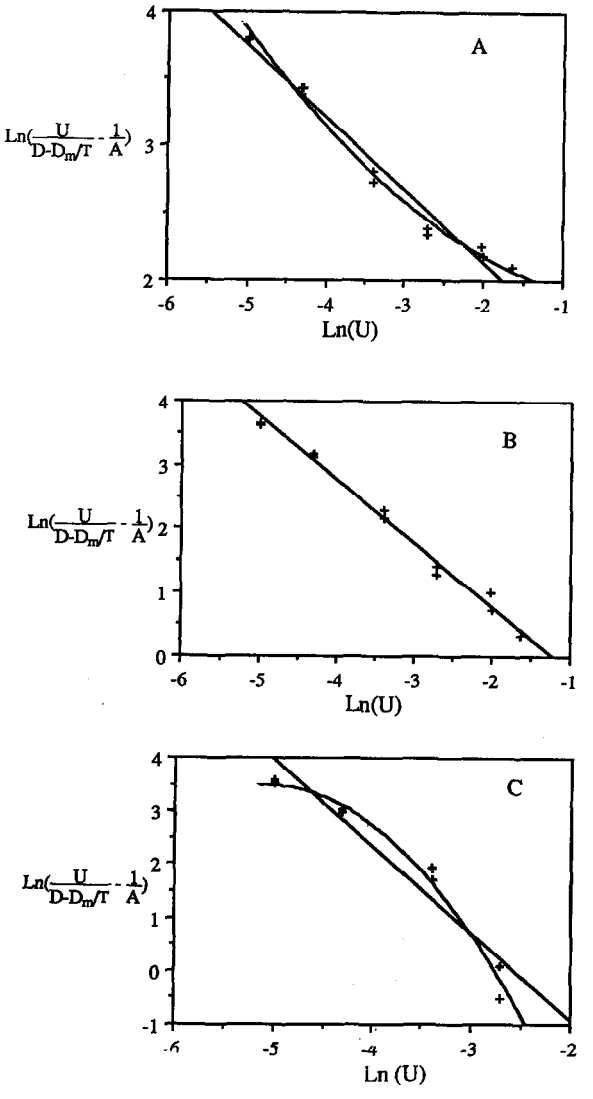

Fig. 5. Z *vs.* $\ln(U)$ plots of the experimental dispersion data with $Z = \ln [U/(D - D_m/T) - 1/A]$ for different values of $1/A$. (A) $1/A = 38.2$; (B) $1/A = 45.0$; (C) $1/A = 48.0$. The straight lines correspond to mean least-square linear regression. The other curves correspond to a second-degree polynomial fit.

demonstrated in Fig. 5, where such plots are shown for three different values of $1/A$. The first two ($1/A = 38.2$ and $1/A = 45.0$) correspond to the slopes given by the linear regression of the experimental (Y, U'') data according to eqn. 22 for $n = 1/2$ and $n = 1$, respectively [for $n = 1/3$, one obtains $1/A = 29.8$, which gives a strongly non-linear (Z, ln U) plot, which, for this reason, is not shown in Fig. 5]. For the sake of comparison, a plot for a larger $1/A$ value ($1/A = 48$) is also shown. Fig. 5 indicates that the curve is concave for relatively low values of $1/A$, then becomes convex for larger

$1/A$ values. Eventually, it becomes linear for a given value of $1/A$. A computer search for the $1/A$ value giving the best linear fit of the data provides $1/A = 45$, which is precisely the value obtained by the procedure mentioned above for $n = 1$. With this $1/A$ value, a linear regression of the (Z, ln U) data gives, for the slope n, a value of 0.994, which, as expected, is very close to 1. Further, this $1/A$ value corresponds to a limiting dispersion length at large Péclet numbers equal to 0.022 cm, *i.e.*, to 1.06 d_p, which as can be seen in Fig. 2 is close to the experimentally obtained value, while the A values obtained by linear regression of eqn. 22 for the Horváth and Lin model ($n = 1/3$, $A = 1.60\ d_p$) and the Huber model ($n = 1/2$, $A = 1.25\ d_p$) are too large.

DISCUSSION

All these results provide a strong indication that eqn. 21 gives a correct representation of the flow dependence of the dispersion length and that the Giddings model with $n = 1$ is the most appropriate model for describing the experimental data. This suggests that, among the five different levels of flow non-uniformities distinguished by Giddings, either only one is affecting significantly the dispersion length or, if two or more of them are influencing this length, they have similar values of A/B (or, equivalently, Λ/C). Indeed, in the latter instance, adding two coupling terms with identical Λ/C values in eqn. 13 is equivalent to multiplying one coupling term by some appropriate constant. One finds, from a linear regression of the experimental data, a Λ value of 1.06, while the values estimated by Giddings are 0.5, 0.5 and 0.1 for the trans-channel, short-range inter-channel and long-range inter-channel effects, respectively. The B value derived by linear regression in Fig. 4C is equal to 3.40 s, corresponding to a C value in eqn. 10 of 0.103. The corresponding C values approximately estimated by Giddings for the three above effects are 0.005, 0.25 and 1, which gives Λ/C values of 100, 2 and 0.1, respectively, while the experimental Λ/C value is 10. From a comparison of these estimated and experimental values it seems that the column does not contain long-range inter-channel non-uniformities, which gives some indication of the quality of the packing procedure. However, the experimental Λ, C and Λ/C values do not correspond closely to the estimated values for either the trans-channel effect or the short-range inter-channel effect. If only one level of flow irregularities is present, as suggested above, it would have to be the trans-channel level which is present even in a crystal-like array of identical spheres. It is difficult, however, to imagine that the short-range inter-channel effect is totally absent because the packing procedure cannot be perfect. These remarks suggest, therefore, that our data reflect some combination of the trans-channel and inter-channel effects and that the Λ/C ratios for these two effects are not as different as the corresponding values estimated by Giddings.

It is of interest to interpret these experimental data by means of the Bouchaud and Georges model, which gives the same flow dependence of the dispersion length as the Giddings model but which is based on a simple geometric construction. This model has three parameters, f, γ and ξ, while the linear regression provides only two coefficients. If one assumes ξ is equal to the particle diameter, d_p, which seems to be a reasonable cell size to be used, then one obtains $f = 0.41$ and $\gamma = 0.11$. As γ is the velocity ratio between the two branches which have been assumed to have the same length, γ represents a permeability ratio and can be assumed to be equal to the ratio of

the squares of the diameters of the two branches, according to the Poiseuille expression. This size ratio is then found to be equal to 1/3. The Bouchaud and Georges model allows the dispersion behaviour of an extremely complex system such as a porous medium to be represented by that of a simple geometric system.

One should not be surprised that the Giddings model provides the best fit to the experimental data. Indeed, the model developed by Huber is not based on a physical model for dispersion but relies on the empirical mass transport correlation by Hiby, the accuracy of which has been questioned[19,20]. Further, this correlation is based on dispersion data obtained for Péclet numbers between 30 and 10^5. This does not allow a full description of the curvature of the l_d *vs.* *Pe* curve associated with the coupling effect for Péclet numbers between 5 and 100.

The discrepancy with the Horváth and Lin equation is even greater than that with the Huber expression. As already noted, this comes, in part, from the fact that the flow-dependent expression according to Pfeffer and Happel[12] for the stagnant boundary layer thickness, on which their equation is based, is only valid at large Péclet numbers and should therefore be used only for $Pe > 50$ (ref. 21). At lower *Pe*, the stagnant layer approaches a constant value and so should the corresponding term in the dispersion length equation. Further, the implicit approximation made in the Horváth and Lin derivation of the volume fraction of the free-streaming fluid [$1/(1 + x) = 1 - x$, where x represents the ratio of the stagnant film volume to the total fluid volume] requires that the stagnant layer is small and thus that *Pe* is large. For these reasons, the Horváth and Lin equation should not be applied for Péclet numbers lower than 50–100. However, it is seen in Fig. 3 that the convex part of the l_d *vs.* *Pe* curve, which reflects the velocity dependence of the flow non-uniformities contribution to the dispersion length, is mainly found for *Pe* values between 5 and 100. It is therefore not surprising that the Horváth and Lin equation cannot fit the experimental data satisfactorily.

Although the Giddings model provides the best fit of the experimental data in this study, one may wonder why it has not been found satisfactory in some previous similar studies with non-retained solutes and non-porous particles. In one of the first experimental proofs of the correctness of the then disputed coupling concept, Knox[22] found that the slope of the log l_d *vs.* log *Pe* curves was much smaller than 1, as a result of the coupling effect. However, he did not find a constant limiting value for l_d at large *Pe* but, instead, that l_d decreased after reaching a maximum value around $Pe =$ 5000–30 000, depending on the experimental conditions. This decrease was attributed to the onset of turbulence at large *Pe*. For all Péclet numbers, the l_d values were significantly affected by the d_c/d_p ratio of the column diameter to particle diameter, which was lower than in the present experiment. One can expect that a low d_c/d_p value will induce, first, a non-random porosity variation across the column radius, as noted by Cohen and Metzner[23] for d_c/d_p values lower than 30 in the case of newtonian fluids and, second, an important trans-column effect and, consequently, a relatively large A value. This can explain why the Knox data are better fitted by a modification of eqn. 13 obtained with an integral form in which A is constant while contributions from different C values are weighted inversely with C. Knox also found that A is of the order of magnitude of the column diameter, rather than of the particle diameter as found in this study.

In their experiments with d_c/d_p values of about 100, as in this present study,

Horváth and Lin found that (l_d, Pe) data in the Pe range 0.5–10 000 are better fitted to eqn. 17 than to eqn. 13 or 15 (ref. 4). One can note that, at large Pe, they obtained l_d values 6–7 times larger than those in Fig. 3, which indicates a significant Λ value. However, the Λ values should be the same for the three models. Therefore, this probably reflects the fact that various levels of flow non-uniformities contribute to peak broadening and that the overall dispersion length is the result of trans-channel, short-range inter-channel, long-range inter-channel and, perhaps, trans-column effects. Then the Λ values of each individual effect add together at large Pe. Further, l_d does not reach a constant value at Pe up to 10 000, which indicates that at least one of these effects is characterized by a very large Λ/C value. Indeed, it can be shown from eqn. 13 that $l_d - 1/TPe$ reaches 90% of its limiting Λ value when Pe is equal to $9\Lambda/C$. In addition, it must be remembered that l_d *vs.* Pe data represent average dispersion data along the column length whereas eqns. 13, 15 and 17 are local expressions of the dispersion length, *i.e.*, of half the rate of increase of the variance of the zone or front per unit column length. If the Péclet number, for instance, is not constant all along the column, then the experimentally measured dispersion coefficient reflects some average value of the dispersion length over the range of Péclet numbers scanned from the inlet to the outlet of the column. In Horváth and Lin's experiments, where the pressure drops at the largest Pe were probably of the order of magnitude of several hundred bars, the pressure dependence of the diffusion coefficient may have led significant variations of Pe along the column. Similar longitudinal gradients in Pe are correctly taken into account in gas chromatography by means of appropriate compressibility factors when they are due to the mobile phase compressibility, but they are generally neglected in liquid chromatography where the experimentally determined dispersion coefficient (or dispersion length) is plotted as a function of the Péclet number calculated using the value of the diffusion coefficient at atmospheric pressure. Such a practice has been shown to induce a significant increase in the apparent dispersion length over the true local value, especially at large Péclet numbers[24].

Finally, it is of interest, for optimization purposes, to note the minimum value of the reduced dispersion length, $l_{d,min}$ and the corresponding Péclet number, Pe_{opt}. From derivation of eqns. 13 and 21 with $n = 1$, one obtains

$$Pe_{opt} = \frac{1}{\sqrt{CT} - \frac{C}{\Lambda}} \tag{29}$$

and

$$l_{d,min} = 2\sqrt{\frac{C}{T}} - \frac{C}{\Lambda T} \tag{30}$$

The coordinates of the optimum appear to be highly sensitive to the values of C but only to a much smaller extent to the value of Λ. This reflects the fact that, at the relatively low Pe corresponding to this minimum, the diffusive mechanism is the most active process for relaxation of the transversal flow inequalities. With the present

values of A (1.06), C (0.103) and $1/T$ (0.6), one obtains $Pe_{opt} = 3.15$ and $l_{d,min} = 0.44$. This minimum dispersion length, which corresponds approximately to the observed minimum in Fig. 3, is about half the value obtained by Horváth and Lin and also the best reported values for high-performance liquid chromatographic (HPLC) columns (reduced plate height of 2). This indicates that there is no precisely defined lower limit for the minimum dispersion length and that it depends strongly on the quality of the packing.

CONCLUSION

The study of the dispersion of a non-retained solute in a column packed with impervious spherical particles and an appropriate data treatment of the experimentally measured values have revealed that the experimental data are correctly fitted by the Giddings coupling equation whereas they deviate from the behaviour predicted by the Huber and, especially, the Horváth and Lin expressions, in spite of the relatively small differences between these equations. This validates the physical model of the coupling of the convective and diffusive transport processes on which the Giddings equation is based.

Although the present study has dealt only with a packing of non-porous particles, this conclusion should also hold for packings of porous particles as the band broadening arising from the interstitial space is believed to be the same for these two kinds of packings.

It must be emphasized that such a conclusion can be drawn because great precautions have been taken to obtain a packing that is as regular as possible and to eliminate, as far as possible, any other source of dispersion than that arising from the flow non-uniformities in the interstitial space of the bed, especially the band broadening contributions associated with the solute retention, the porous space inside the particles, the thermal effect due to the viscous dissipation and the pressure dependence of the diffusion coefficient.

In liquid chromatographic columns packed with small porous particles, all these effects will give a more or less pronounced contribution to the overall dispersion. In addition, the usual packing procedure with these columns (filtration under pressure of a slurry of particles) probably leads to a longitudinal porosity gradient which may affect the scale and the amplitude of the flow non-uniformities and also induce a longitudinal cross-sectional average velocity gradient. Hence, the actual dispersion length is continuously changing along the column and the experimentally determined value corresponds to some average column length. This provides some explanation of the fact that HPLC experiments have not allowed the models to be distinguished. Accordingly, in kinetic optimization studies of the experimental HPLC conditions for which a relationship between dispersivity and flow velocity is required, a semi-empirical dispersion equation such as the Knox equation[25], in which the relatively complicated coupling term for the dispersion length in the interstitial space is replaced with a simple Pe^m ($m \approx 1/3$) expression, will generally be satisfactory.

ACKNOWLEDGEMENT

Fruitful discussions with Jean-Pierre Hulin are greatly appreciated.

REFERENCES

1 J. C. Giddings, *Dynamics of Chromatography*, Marcel Dekker, New York, 1965.
2 J. F. K. Huber and J. A. R. J. Hulsman, *Anal. Chim. Acta*, 38 (1967) 305.
3 J. F. K. Huber, *J. Chromatogr. Sci.*, 7 (1969) 85.
4 Cs. Horváth and H.-J. Lin, *J. Chromatogr.*, 126 (1976) 401.
5 M. Martin, unpublished results.
6 K. H. Coats and B. D. Smith, *Soc. Pet. Eng. J.*, March (1964) 73.
7 P.-Z. Wong, J. Koplik, J. P. Tomanic, *Phys. Rev. B*, 30 (1984) 6606.
8 J. N. Roberts, L. M. Schwartz, *Phys. Rev. B*, 31 (1985) 5990.
9 J. J. van Deemter, F. J. Zuiderweg and A. Klinkenberg, *Chem. Eng. Sci.*, 5 (1956) 271.
10 J. W. Hiby, in P. A. Rottenburg (Editor), *Proceedings of the Symposium on Interaction between Fluids and Particles*, Institution of Chemical Engineers, London, 1962, p. 312.
11 J. Happel, *AIChE J.*, 4 (1958) 197.
12 R. Pfeffer and J. Happel, *AIChE J.*, 10 (1964) 605.
13 D. L. Koch and J. F. Brady *J. Fluid Mech.*, 154 (1985) 399.
14 A. Acrivos and T. D. Taylor, *Phys. Fluids*, 5 (1962) 387.
15 P. G. Saffman, *J. Fluid Mech.*, 6 (1959) 321.
16 J.-P. Bouchaud and A. Georges, *C.R. Acad. Sci., II*, 307 (1988) 1431.
17 J.-P. Bouchaud, personal communication.
18 R. C. Weast (Editor), *Handbook of Chemistry and Physics*, CRC Press, Boca Raton, FL, 60th ed. 1979–80, p. F-62.
19 R. S. Deelder, *J. Chromatogr.*, 47 (1970) 307.
20 R. Tijssen, *Ph.D. Thesis*, Technical University of Delft, 1979, p. 12.
21 F. H. Arnold, H. W. Blanch and C. R. Wilke, *J. Chromatogr.*, 330 (1985) 159.
22 J. H. Knox, *Anal. Chem.*, 38 (1966) 253.
23 Y. Cohen and A. B. Metzner, *AIChE J.*, 27 (1981) 705.
24 M. Martin and G. Guiochon, *Anal. Chem.*, 55 (1983) 2302.
25 J. N. Done, G. J. Kennedy and J. H. Knox, in S. G. Perry (Editor), *Gas Chromatography 1972*, Applied Science, London, 1972, p. 145.